A New Thermal Model of an Angular Contact Ball Bearings, in a Standard Arrangement, subjected to Radial Loads, based on State Variables and Control Volumes

Sebastian Cabezas[1], György Hegedűs[2] and Péter Bencs[3]

[1,2] Institute of Machine Tools and Mechatronics, Faculty of Mechanical Engineering and Information Technology, University of Miskolc, 3515 Miskolc-Egyetemváros, Hungary
E-mails: szgtscab@uni-miskolc.hu, hegedus.gyorgy@uni-miskolc.hu

[3] Institute of Energy Engineering and Chemical Machinery, Faculty of Mechanical Engineering and Information Technology, University of Miskolc, 3515 Miskolc-Egyetemváros, Hungary, E-mail: peter.bencs@uni-miskolc.hu

Abstract: Permanent or temporary failures in bearing systems are often caused by excessive or prolonged heat generation, within an angular contact ball bearing, during operations arising from external loads. Considering the complexity of getting experimental thermal measurements in an angular ball bearing arrangement, analytical techniques must be utilized in order to predict the thermal behavior thereof, taking into account variables such as rotational speed, the type of load and the operational conditions. The aim of this study is the development of a thermal model applying the state-space approach, able to predict thermal characteristics of an angular contact ball bearing in standard arrangement subjected to radial loads. For this purpose, an angular ball bearing, model 7203BEP, in standard arrangement, was treated as the representative model. The arrangement was divided into three independent control volumes, these are, the inner-race, the ball and the outer-race/housing. Thereafter, the energy equation and the theory of rolling contact heat transfer are utilized to determine heat fluxes and temperature variations between the contact regions. The thermal resistances developed between the ball/ inner-race, outer-race/ ball, inner-race/ shaft and outer-race/ housing were calculated as variables depending on the rotational speed, wherewith the thermal analysis is performed. Space variables including, temperature of the inner-race T_i, temperature of the balls T_b and temperature of the outer-race/ housing T_{oh} were calculated and the results were compared by Finite Element Analysis simulations using Ansys transient thermal software. The findings herein, show that the maximum value of mean deviation of temperature obtained with the proposed thermal model and the Finite Element Analysis (FEM) simulations was less than $sd < 3.50\%$, hence, indicating that the model is in good agreement with the numerical solutions. In this manner, the presented thermal model can be utilized, as an observer, to predict the thermal behavior, in different types of angular contact ball bearings, that undergo radial loads. Furthermore,

the thermal model provides relevant information for further studies, related to thermal distribution in machine components.

Keywords: Angular ball bearing; thermal model; thermal resistance; state-space approach; state variables

Nomenclature

a Ellipse major axis (mm)

A_b Surface area of the ball (m^2)

A_i Surface area of the inner-race (m^2)

A_o Surface area of the outer-race (m^2)

b Ellipse minor axis (mm)

c_p Specific heat $(\mathrm{J/kgK})$

d_m Mean diameter (mm)

E Young's modulus $(\mathrm{N/mm}^2)$

F External load (kN)

F_t Applied force (kN)

F_r Radial force (kN)

G_{rr} Bearing type and load factor.

h_l Lubricant coefficient $(\mathrm{W/m^2K})$

k Thermal conductivity $(\mathrm{W/mK})$

m_b Mass of the ball (kg)

m_i Mass of the inner-race (kg)

m_{oh} Mass of the outer-race/ housing (kg)

M_{fr} Rolling frictional moment (Nmm)

n Rotational speed (rpm)

N Number of balls

$\dot{Q}_{bi}$ Heat generated from the ball to the inner-race (W)

R_{is} Thermal resistance between the inner-race and the shaft $(\mathrm{K/W})$

R_{ob} Thermal resistance between the outer-race and the ball $(\mathrm{K/W})$

R_{oh} Thermal resistance of the outer-race/ housing $(\mathrm{K/W})$

t Time (s)

T_b Temperature of the ball $(^\circ\mathrm{C})$

T_{bii} Initial temperature of the ball $(^\circ\mathrm{C})$

T_h Temperature of the housing $(^\circ\mathrm{C})$

T_i Temperature of the inner-race $(^\circ\mathrm{C})$

T_{ii} Initial temperature of the inner-race $(^\circ\mathrm{C})$

T_{is} Initial temperature of the shaft $(^\circ\mathrm{C})$

T_l Temperature of the lubricant $(^\circ\mathrm{C})$

T_o Temperature of the outer-race $(^\circ\mathrm{C})$

T_{ohi} Initial temperature of the outer-race/ housing $(^\circ\mathrm{C})$

T_s Temperature of the shaft $(^\circ\mathrm{C})$

V Tangential speed $(\mathrm{m/s})$

$\dot{Q}_{bl}$ Heat by convection between the ball and the lubricant (W)

$\dot{Q}_{f}$ Total friction heat generation (W)

$\dot{Q}_{fb}$ Frictional heat into the ball (W)

$\dot{Q}_{fi}$ Frictional heat into the inner-race (W)

$\dot{Q}_{fo}$ Frictional heat into the outer-race (W)

$\dot{Q}_{il}$ Heat by convection between the inner-race and lubricant (W)

$\dot{Q}_{oh}$ Heat generated through the outer-race/housing (W)

$\dot{Q}_{ol}$ Heat by convection between the outer-race and lubricant (W)

R Thermal resistance $\left(\mathrm{K/W}\right)$

R_{bi} Thermal resistance between ball and the inner-race $\left(\mathrm{K/W}\right)$

α Contact angle $\left(^{\circ}\right)$

α_{d} Thermal diffusivity $\left(\mathrm{m^2/s}\right)$

γ Poisson's ratio

μ Geometric factor 1. Ref.[10]

υ Lubricant kinematic viscosity $\left(\mathrm{mm^2/s}\right)$

ρ Density $\left(\mathrm{kg/m^3}\right)$

ρ_{c} Radii of curvature (mm)

ν Geometric factor 2. Ref [10]

Φ_{is} Inlet shear heating reduction factor. Ref. [10]

Φ_{rs} Starvation reduction factor. Ref. [10]

Subscripts:

b Ball

i Inner-race

o Outer-race

oh Outer-race/ housing

1 Introduction

The performance of rotary machines leans on diverse factors, including the appropriate thermal conditions of rolling elements. The operational capability of the bearing might be affected by a sudden increase of temperature, mostly occasioned by friction among the elements comprising a rolling bearing. Although, rolling bearings have been called non-frictional elements [1], it is well known that rolling contact produces frictional moments, thereby generating the phenomena of heat transfer [2]. The thermal efficiency of a bearing arrangement will depend on its capacity to dissipate heat among the bearing components and the adjacent elements. Frictional moments depend on sundry variables, among them, the applied load, operating speeds, lubricant type, bearing arrangement, type of bearing, environmental conditions [1] and the determination of frictional moments is

substantiated by the Hertzian contact theory [3]. In order to enhance thermal analysis in bearings and knowledge thereof, for decades, a vast number of important investigations have been conducted, including the creation and utilization of computational tools to predict life and performance of bearings [4] and the development of mathematical expressions relating friction-power for specific types of bearings [5]. To mention some remarkable investigations regarding thermal behavior in bearings, J. L. Stein et al. [6] developed a dynamic mathematical model as the basis of an observer, so that bearing internal force can be on-line monitored based on easy to measure spindle system quantities, such as bearing temperature and spindle-speed. K. Mizuta et al. [7], studied heat transfer characteristics between the inner and outer ring measured experimentally, and the effect of balls as a heat carrier was calculated theoretically. T. Sibilli et al. [8], compared a thermal network model and a finite element model of an experimental high-pressure shaft ball bearing and housing in order to provide a template for predicting temperatures and heat transfer for a variety of bearing models. Z. De-xing et al., estimated thermal performances with an optimized thermal grid model for a pair of front bearings mounted in a high-speed spindle. The results show that the deviation between the calculation and experimental measurements was 9%, which can be beneficial for operating accuracy and service life as bearing temperature rise can be forecasted [9]. The construction of experimental rigs presents various difficulties including, the location of temperature sensors in rotating elements, the accessibility to the inner parts of the bearing arrangement, the application of external radial, axial loads or a combination of both by external sources, the analysis of the lubrication regime wherewith the bearing is tested. Therefore, the utilization of the different computational, analytical and numerical techniques must be considered valid approaches to determine solutions, as long as these solutions have been tested or compared. At present, bearing manufacturers have developed equations and mathematical expressions to calculate frictional moments and are publicly issued in order to facilitate their utilization by engineers and researchers. Detailed information thereof, can be found in [10] [11].

Having said that, this paper presents a thermal model utilizing the state-space method and control volumes, capable of observing temperature differences in an angular contact ball bearing type SKF 7203 BEP mounted in a back-to-back (DB) arrangement, which is subjected to radial loads ranging from $0.75 – 7.5\,\text{kN}$

$0 – 4000\,\text{rpm}$, taking into account the speed limits of conventional electric motor capabilities employed in bearing experimental testing rigs. The findings obtained with the proposed thermal model were compared with Finite Element Analysis (FEA) using Ansys transient thermal. The mean deviations between FEA simulations and the thermal model were calculated,

$sd = 1.40$ for the outer-race /housing temperature T_{oh}, $sd = 1.64$ for the ball temperature T_b and $sd = 1.40$ for the inner-race temperature T_i. Considering that the values of mean deviation are low, the thermal model is in accordance with numerical simulations. The present work aims to provide a practicable analytical tool wherewith the thermal behavior of the bearing components and adjacent elements thereof are observed, hence providing an intuitive and straightforward methodology that can be applied to bearings with similar geometries under mechanical forces alike.

2 Materials and Methods

Figure 1 illustrates the assembly model and a cross-sectional view of a DB back-to-back bearing arrangement subjected to radial loads exerted by an external source.

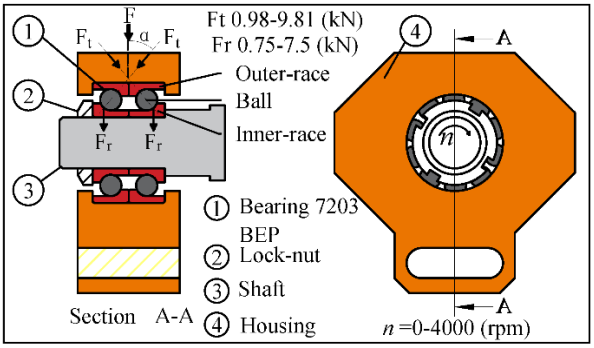

Figure 1
Scheme of an angular contact bearing in standard arrangement (Source: Author)

The assembly consists of four elements, the housing, in which the bearings are packed and the external load can be applied; the SKF 7203 angular contact ball bearing, in which heat is dissipated; the lock-nut, which fastens and supports the assembly; and the shaft. The development of the thermal model was divided into four stages, load model, frictional model, heat generation model and state-space variables model.

2.1 Load Model

Angular contact ball bearings are suitable for working under different types of loads, including axial loads, radial loads, combinations of axial and radial loads, preload in the axial direction, preload in radial direction, centrifugal forces [1, 6, 9], consequently, this type of bearing is widely used in high-speed machining

applications. It is important to consider that each type of load will produce different effects with regards to heat transfer and other phenomena such as vibrations. This research focuses on the thermal effects caused by pure radial loads, determining them depends on the applied force by the external source and the bearing contact angle, hence the radial force F_r is obtained using Equation (1) [1].

$$F_r = F_t \cdot \cos(\alpha) \tag{1}$$

2.2 Frictional Model

Heat transfer in angular contact ball bearings is associated not only with motion and the thermal physical properties of the bodies under rolling contact (inner-race and ball, outer-race and ball), but with the size and shape of the contact region [2]. Moreover, according to Hertzian contact theory, the pressure between two elastic bodies in contact will form an ellipse of major axis a and minor axis b as shown in Figure 2, which can be calculated using Equation (2) [2].

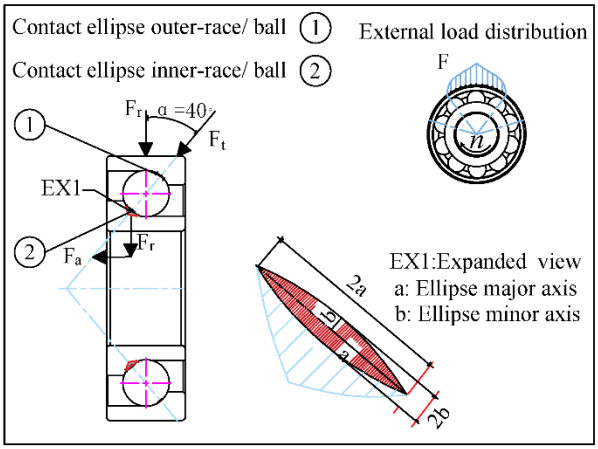

Figure 2
Force distribution and contact region (Source: Author)

$$a = \mu \cdot \left[\frac{3\left(1-\frac{1}{\gamma^2}\right)\frac{F_r}{\cos(\alpha)}}{E\sum\rho_c} \right]^{1/3}$$
$$b = \upsilon \cdot \left[\frac{3\left(1-\frac{1}{\gamma^2}\right)\frac{F_r}{\cos(\alpha)}}{E\sum\rho_c} \right]^{1/3} \tag{2}$$

As defined in the Introduction, nowadays bearing manufacturers provide mathematical models to determine frictional moments that follow real behavior of the bearings, considering the contact area and the internal and external factors. Inasmuch as in this paper a bearing model SKF 7203 BEP is being used, the rolling frictional moment was determined utilizing its proper mathematical model given by Equation (3) [10].

$$G_{rr} = 4.33 \cdot 10^{-7} \cdot d_m^{1.97} \left[F_r + 2.44 \cdot 10^{-12} d_m^4 n^2 + 2.02 F_t \cdot \sin(\alpha) \right]^{0.54}$$
$$M_{fr} = \Phi_{is} \Phi_{rs} G_{rr} \left(\nu n \right)^{0.6} \tag{3}$$

Equation (3), relates the effect of radial and axial forces, starvation factor, geometrical specifications of the angular bearing, rotational speed and the operating viscosity of the lubricant. For detailed information on the calculation method, revise reference [10]. The relation of the frictional moment and the rotational speed at different radial loads is presented in Figure 3.

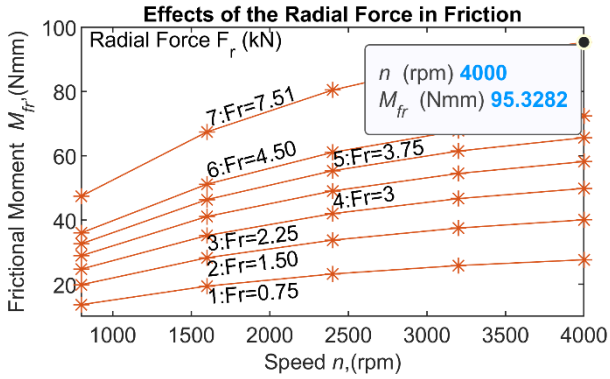

Figure 3
Frictional moment M_{fr} vs. rotational speed n

Figure 3 shows that the frictional moment M_{fr} increases in a non-linear behavior when the rotational speed n increases. This effect will directly influence the heat generation throughout the bearing and its adjacent components.

2.3 Heat Transfer Model

As in all phenomena of heat transfer, the dissipation of heat in angular bearings happens following the principles of distribution of thermal energy occurring due to spatial temperature differences [1] [12], and can be mathematically approached by heat transfer modes. Mostly, heat is generated by friction due to rolling contact (between the inner-race and balls, outer-race and balls). By conduction, heat is dissipated between the contact regions (inner-race, balls, outer-race, housing).

By convection, heat is dissipated between fluids or gases and solid bodies (oil-lubricant and balls, oil-lubricant and races). In some special bearing applications such as aerospace or high-temperature applications, might be useful to analyze heat transfer by radiation. Once the frictional moment is calculated, it is necessary to divide the structure arrangement shown in Figure 1 in a suitable way, thereby avoiding the presence of more unknown variables than equations to find solutions. This approach is achieved by selecting appropriate control volumes, it means, selecting a region of space bounded by a control surface through which heat is flowing [13]. On this application, the bearing arrangement was divided into three parts: the inner-race, which is a non-static part, exchanges heat with the balls, the lubricant and the shaft; the balls, which are a non-static part and exchange heat with the inner-race, lubricant, and outer-race; the outer-race/ housing which is a static part and exchanges heat with the balls, lubricant and the surroundings. Considering that the applied load is carried by the housing, the distribution of heat is conceived is illustrated in Figure 4.

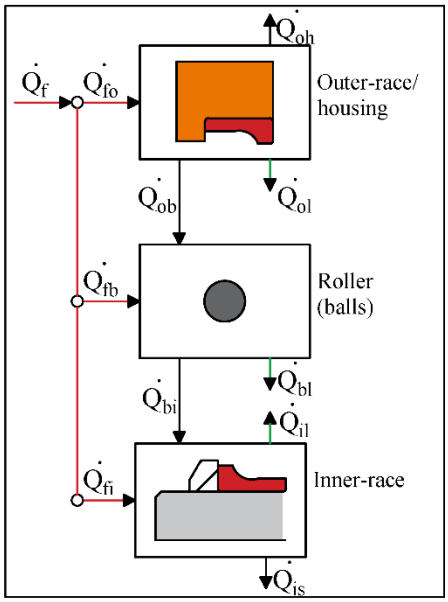

Figure 4
Heat transfer block diagram (Source: Author)

The total friction heat flow $\dot{Q}_f$ [4] is obtained utilizing the power loss formula which relates the rotational speed n and the frictional moment M_{fr} [2].

$$\dot{Q}_f = 1.5 \cdot 10^{-4} \cdot M_{fr} \cdot n \tag{4}$$

A fully lubricant film between the rings and the balls is developed, hence separating the surfaces and allowing the functionality of the bearing under the manufacturer specifications. Heat by friction occurs at the contact surfaces and then is distributed to the inner-race $\dot{Q}_{fi}$, spheres $\dot{Q}_{fb}$ and outer-race $\dot{Q}_{fo}$ [6]. Since the rolling elements are designed to absorb most of the distributed load [1], it is established that 50% of the total power losses by friction is absorbed by the rolling elements (balls), the rest is divided between the inner-race 25% and outer-race 25% of the total power losses as stated in Equation (5) [6].

$$\begin{aligned} \dot{Q}_{fb} &= 0.5 \cdot \dot{Q}_f \\ \dot{Q}_{fi} &= 0.25 \cdot \dot{Q}_f \\ \dot{Q}_{fo} &= 0.25 \cdot \dot{Q}_f \end{aligned} \tag{5}$$

The relation between the power losses and the rotational speed for different radial loads is shown in Figure 5. The figure shows that the total heat Q_t increases exponentially with regards to the rotational speed n and the radial load F_r.

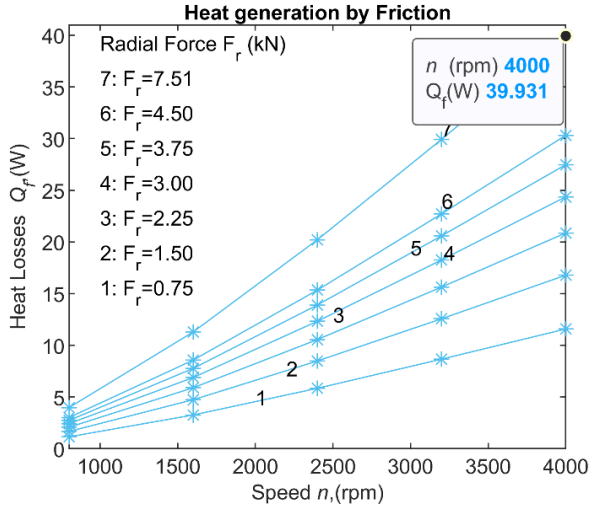

Figure 5

Heat losses $\dot{Q}_f$ vs. rotational speed n

Heat by conduction is transferred between the spheres and inner-race $\dot{Q}_{bi}$, inner-race and the shaft $\dot{Q}_{is}$, outer-race and spheres $\dot{Q}_{ob}$ and through the outer-race and housing $\dot{Q}_{oh}$ [6].

The formulas are:

$$\begin{aligned}
\dot{Q}_{bi} &= \frac{\left(T_b - T_i\right)}{R_{bi}} \\
\dot{Q}_{is} &= \frac{\left(T_i - T_{sh}\right)}{R_{is}} \\
\dot{Q}_{ob} &= \frac{\left(T_o - T_b\right)}{R_{ob}} \\
\dot{Q}_{oh} &= \frac{\left(T_o - T_h\right)}{R_{oh}}
\end{aligned} \tag{6}$$

The thermal resistances R_{bi}, R_{ob} for rotating elements, depend on the tangential speed, the Hertzian contact area, the thermal conductivity and the thermal diffusivity [5], and are obtained using Equation (7) [5].

$$R = \frac{0.8}{N \cdot b \cdot k}\left(\frac{\pi \cdot \alpha_d}{a \cdot V}\right)^{1/2} \tag{7}$$

Figure 6, illustrates the relation of the thermal resistances with respect to the rotational speed. It is noticeable that the thermal resistances between the contact regions R_{bi} and R_{ob} decrease with respect to the rotational speed n, hence heat dissipation by conduction between the contact regions will increase.

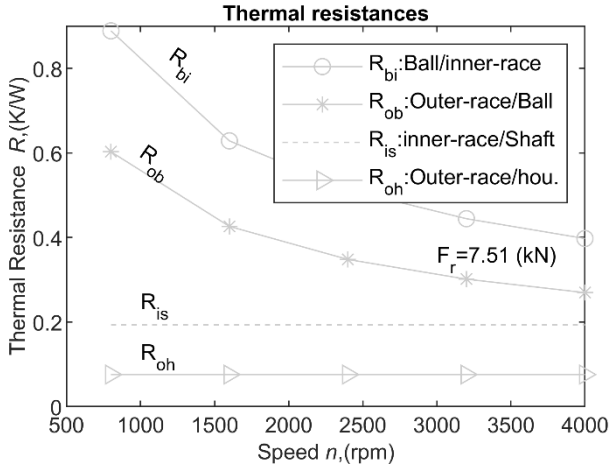

Figure 6
Thermal resistances $R,(\mathrm{K/W})$

Heat by convection is dissipated between the inner-race and the lubricant $\dot{Q}_{il}$, balls and the lubricant $\dot{Q}_{bl}$, and outer-race and lubricant, $\dot{Q}_{ol}$, and are calculated using Equation (8) [6].

$$\begin{aligned}\dot{Q}_{il} &= h_l \cdot A_i \cdot (T_i - T_l)\\ \dot{Q}_{bl} &= h_l \cdot A_b \cdot (T_b - T_l)\\ \dot{Q}_{ol} &= h_l \cdot A_o \cdot (T_o - T_l)\end{aligned} \tag{8}$$

The temperature variations along the surfaces of the inner-race T_i, ball T_b and outer-race/ housing T_{oh} are calculated applying the energy equation to the three control volumes as follows:

$$\begin{aligned}m_i \cdot c_p \cdot \frac{\partial T_i}{\partial t} &= \dot{Q}_{fi} + \dot{Q}_{bi} - \dot{Q}_{il} - \dot{Q}_{is}\\ m_b \cdot c_p \cdot \frac{\partial T_b}{\partial t} &= \frac{1}{N}(\dot{Q}_{fb} + \dot{Q}_{ob} - \dot{Q}_{bi} - \dot{Q}_{bl})\\ m_{oh} \cdot c_p \cdot \frac{\partial T_{oh}}{\partial t} &= \dot{Q}_{fo} - \dot{Q}_{ob} - \dot{Q}_{ol} - \dot{Q}_{oh}\end{aligned} \tag{9}$$

2.4 State-Space Model

Equation (9), cannot be solved by conventional algebraic methods since there will be more unknown variables than equations. On that account, this paper presents a steady-space approach wherewith modelling and observing a system can be done selecting appropriate state-variables and input-variables sufficient to describe the complete behavior of the system. The state-variables are the temperature of the inner-race T_i, the temperature of the balls T_b and the temperature of the outer-race/ housing T_{oh}. The input variables have been selected meticulously in order to obtain appropriate results. The input variables must be easily measurable by external sensors or calculated by mathematical expressions, and can be selected to suit the problem [14]. Therefore, the power losses by friction $\dot{Q}_f$ which depends on the applied load, rotational speed, lubrication-regime together with temperature of the outer-race T_o were chosen as input-variables. Hence, the description of the system using state-space approach is given by Equation (10).

$$\begin{bmatrix} m_i \cdot c_p \dot{T}_i \\ m_b \cdot c_p \dot{T}_b \\ m_{oh} \cdot c_p \dot{T}_{oh} \end{bmatrix} = \begin{bmatrix} -\left(\frac{1}{R_{bi}} + \frac{1}{R_{is}} + h_l A_i\right) & \frac{1}{R_{bi}} & 0 \\ \frac{1}{N \cdot R_{bi}} & -\frac{1}{N}\left(\frac{1}{R_{ob}} + \frac{1}{R_{bi}} + h_l A_b\right) & 0 \\ 0 & \frac{1}{R_{ob}} & -\frac{1}{R_{oh}} \end{bmatrix} \cdot \begin{bmatrix} T_i \\ T_b \\ T_{oh} \end{bmatrix} + \begin{bmatrix} 0.25 & 0 \\ 0.5 & \frac{1}{N \cdot R_{ob}} \\ 0.25 & \left(\frac{1}{R_{bi}} + h_l A_o\right) \end{bmatrix} \cdot \begin{bmatrix} \dot{Q}_f \\ T_o \end{bmatrix}$$

$$y = \begin{bmatrix} 1 & 0 & 0 \\ 0 & 1 & 0 \\ 0 & 0 & 1 \end{bmatrix} \cdot \begin{bmatrix} T_i \\ T_b \\ T_{oh} \end{bmatrix} \tag{10}$$

Although the system mathematically is controllable, it is important to remark that the proposed model only serves as an observer, it means that the state-variables at $t = t_0$ can be exactly determined from observation of the output over a finite time interval. Further details about controllability and observability are described in reference [14].

3 Results

In this section, the determination of the temperature fields of the three control volumes (inner-race T_i, ball T_b, outer-race/ housing T_{oh}), is presented. The solutions were analyzed utilizing the proposed thermal model given in Equation (9), and finite element analysis simulations.

3.1 Sate-Space Model Solution

The state-space system wherein the state variables T_i, T_b and T_{oh} are analyzed, was determined using MATLAB. The thermal properties of the materials comprising the angular bearing, the initial temperatures of the shaft T_{ish}, oil-mist T_l, inner-race T_{ii}, balls T_{bii} and outer-race/ housing T_{ohi}, are given in Table 1. The geometric specifications of the angular ball bearing necessary to find numerical solutions can be found in the manufacturer's reference [10].

The interval time t is set up until reaching steady-state conditions. The interval time of the thermal analysis for the inner-race and the balls was set up at $t = 30\,s$. For the outer-race/housing was set-up at $t = 300\,s$. The responses of the state-space thermal model are shown in Figure 7 for the inner-race; Figure 8, for the balls and Figure 9 for the outer-race/housing.

Table 1
Thermal properties and initial conditions

Thermal Property	Initial Condition
Thermal conductivity	$k = 46.6(\mathrm{W/mK})$
Poisson's ratio	$\gamma = 0.27$
Specific heat	$c_p = 460(\mathrm{J/kgK})$
Density	$\rho = 7810(\mathrm{kg/m^3})$
Oil mist convection coefficient	$h_l = 409(\mathrm{W/m^2K})$
Initial temperatures	$T_{ish} = 25(^\circ C), T_{ii} = 26.5(^\circ C), T_{ohi} = 25(^\circ C)$ $T_{bii} = 25(^\circ C), T_l = 25(^\circ C)$
Applied radial force	$F_r = 7.5(\mathrm{kN})$
Rotational speed	$n = 0 - 4000$ (rpm)

Due to radial loads, frictional moments are developed between the inner-race and the ball. Part of the heat energy is absorbed in the inner-race and part is dissipated to the lubricant film. During the interval time $t = 30\,s$, applying the operational conditions for the radial force and rotational speed given in Table 1, a temperature increment $\Delta T_i = 5.24\,^\circ C$ occurs in the inner-race as shown in Figure 7.

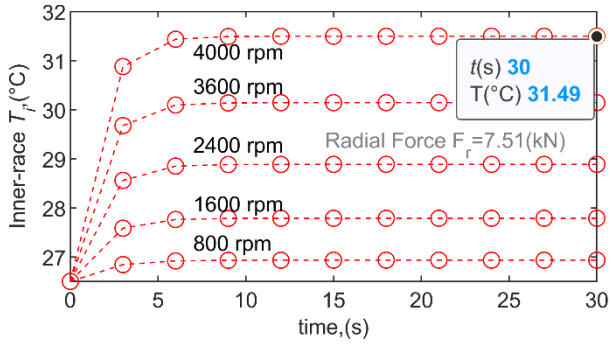

Figure 7
Temperature distribution of the inner-race T_i

An important function of the balls is to distribute the loads uniformly through the bearing components. Considering that most of the frictional moment is absorbed by the balls, it is noteworthy that a high temperature increment $\Delta T_b = 27.50\,^\circ C$ during $t = 30\,s$ occurs, as shown in Figure 8.

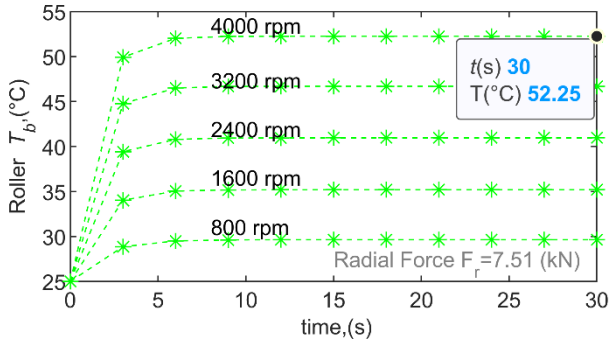

Figure 8
Temperature distribution of the balls T_b

Since the volume comprising in the outer-race/ housing arrangement is bigger compared to the balls and inner-race, very low temperature increments occur at $t = 30\,s$ Consequently, more time is required to reach steady-state conditions. A temperature increment $\Delta T_{oh} = 21.23\,^{\circ}C$ occurs at $t = 300\,s$ as depicted in Fig. 9.

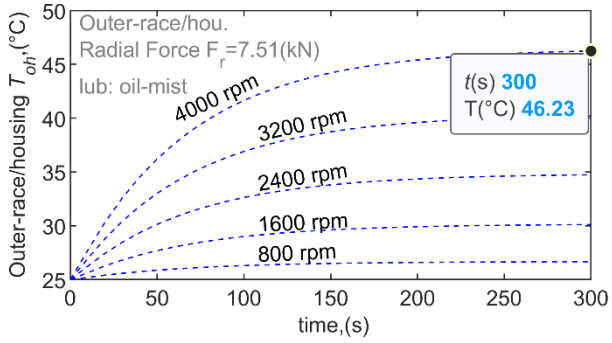

Figure 9
Temperature distribution of the outer-race/ housing T_{oh}

3.2 Finite Element Analysis

To demonstrate the applicability of the proposed thermal model, FEA simulations were performed using ANSYS transient thermal software, for each of the control volumes. The initial conditions for the temperatures are given in Table 1, the time set up for the analysis is the same applied in the previous section. With the aim to obtain more accurate values, the mesh elements were selected **as tetrahedrons of 0.0001 mm size for the inner-race and spheres** as shown in Figure 10 and Figure 11, **and tetrahedrons of 0.01 mm size for the outer-race/housing** as

shown in Figure 12. In the case of the outer-race/ housing, the mesh can be smaller considering that it is a fixed assembly and using small size elements as in the two other control volumes is not relevant.

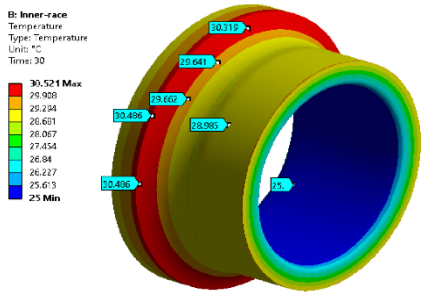

Figure 10
FEA thermal simulation of the inner-race T_i

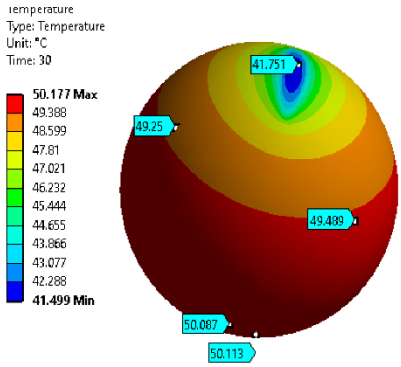

Figure 11
FEA thermal simulation of the ball T_b

Figure 11 illustrates a clear temperature distribution in the rolling elements, starting from the heat dissipation in the Hertzian contact region and distributing the heat through the ball.

Figure 12 illustrates that the most heated part of the outer-race/housing assembly is the region of contact between the balls and the outer-race. Furthermore, this figure also depicts that the housing is the least heated part of the assembly.

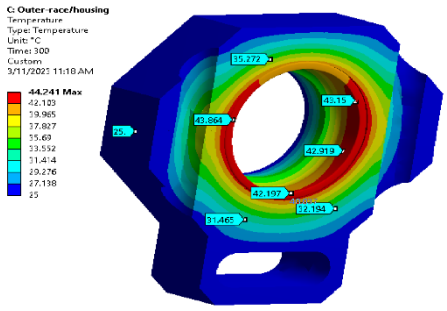

Figure 12
FEA thermal simulation of the outer-race/ housing T_{oh}

The temperature distribution using the proposed thermal and the finite element analysis simulations is presented in Figure 13.

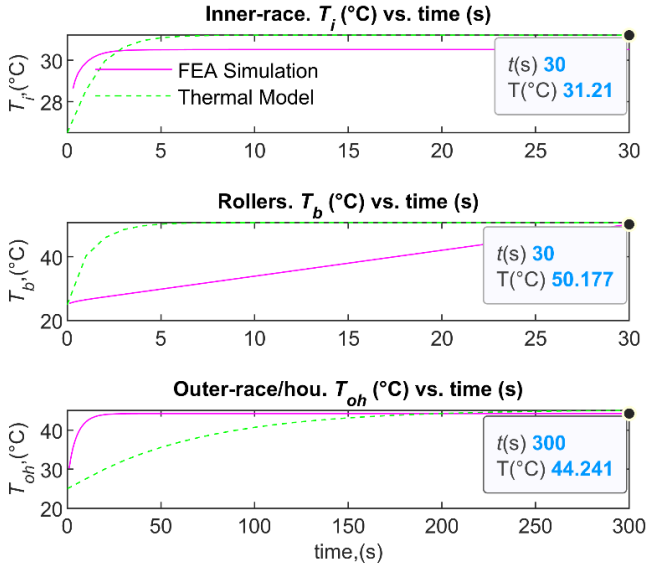

Figure 13
Temperature distribution. Thermal model and FEA simulations

As depicted in Figure 13, the thermal behavior for the inner-race T_i and outer-race/housing T_{oh} regarding the FEA simulations and the thermal model, present similar thermal behavior and it is clearly seen that during the established period of time, the final mean values do not differ prominently. In the case of the balls, the thermal behavior T_b for the FEA simulation exhibit a linear behavior as compared to the behavior obtained for the thermal model. However, the final values at the end of the specified time, do not differ prominently.

Table 2 presents the results of the thermal model and FEA simulations, including the percentage of deviation between both results and the average temperature and the temperature increment from the initial temperatures.

Table 2
Thermal Model and FEA Analysis comparison at $n = 4000\,(\text{rpm})$ $F_r = 7.51\,(\text{kN})$

Control Volume	$\boldsymbol{t}$, **(s)**	**Thermal Model** (℃)	**FEA sim.** (℃)	**Temp. difference** (℃)	**Temp. increment** $\Delta \boldsymbol{T}$ (℃)	**Dev.** $\boldsymbol{sd}$
Inner-race	30	31.49	30.52	0.97	5.24	0.68
Balls	30	52.50	50.17	2.30	27.50	1.64
Outer-race/housing	300	46.23	44.24	1.9	21.23	1.40

Conclusions

A thermal model to predict temperature variations for an angular contact ball bearing, in back-to-back arrangement, subjected to radial loads, using a state-space approach was presented in this paper. The assembly was divided into three control volumes, inner-race, balls and outer-race/ housing. Two best suited input-variables for the state-space model were selected, as the frictional heat $\dot{Q}_f$ (which depends on the applied load, rotational speed, lubrication regime, geometry of the bearing) and the temperature of the outer-race T_o. It could be seen that the thermal resistances between the ball and the inner-race R_{bi} and between the outer-race and the ball R_{ob} decrease, when the rotational speed n increases, in this sense, the heat dissipation rates increase. The thermal resistances of the outer-race/ housing R_{oh}, inner-race and shaft remain constant R_{is}. The output-variables T_i, T_b, T_{oh} which represent the temperature of three control volumes were solved analytically by finding temperature responses with initial conditions at $t = t_0$. The temperature distribution of the inner-race T_i, balls T_b and outer-race/ housing T_{oh}, were determined by the proposed thermal model and were compared by FEA simulations.

The maximum mean deviation between the thermal model and the Finite Element Analysis simulations was found in the balls and was $sd = 1.64$. For the case of the inner-race and outer-race/housing, they were $sd = 0.68$ and $sd = 1.40$ respectively. Since the values of the mean deviation are low, it is said that the thermal model is in good agreement with numerical models and can be used to predict thermal behavior in angular bearings.

The presented model is controllable and observable; however, in this research, the model's importance lies in its observability, as temperature behavior can be predicted analytically. The presented methodology is conceived, aiming to be used in the academic and industrial fields related to machine-tools and other types of machinery, wherein the thermal effects are of enormous importance and need continuous analysis.

References

[1] T. A. Harris and M. N. Kotzalas, Rolling Bearing Analysis. Advanced Concepts of Bearing Technology, Taylor and Francis Group, 5th Edition, 2006

[2] A. Bejan, Theory of rolling contact heat transfer, Journal of Heat Transfer, Vol. 111, No. 2, pp. 257-263, 1989, https://doi.org/10.1115/1.3250672

[3] L. Houpert, An Engineering Approach to Hertzian Contact Elasticity - Part I, Journal of Tribology, Vol. 123, No. 3, pp. 582-588, 2001, https://doi.org/10.1115/1.1308043

[4] R. J. Parker, Comparison of Predicted and Experimental Thermal Performance of Angular Contact Ball Bearings, NASA Technical Paper, No. 2225, 1984

[5] R. A. Burton and H. E. Staph, Thermally Activated Seizure of Angular Contact Bearings, Tribology Transactions, Vol. 10, No. 4, pp. 408-417, 2008, 10.1080/05698196708972200

[6] J. L. Stein and J. F. Tu, A State-Space Model for Monitoring Thermally Induced Preload in Anti-Friction Spindle Bearings of High-Speed Machine Tools, Journal of Dynamic Systems, Measurement and Control, Vol. 116, No. 3, pp. 372-386, 1994, https://doi.org/10.1115/1.2899232

[7] K. Mizuta, T. Inoue, Y. Takahashi, S. Huang, K. Ueda and H. Omokawa, Heat Transfer Characteristics Between Inner and Outer Rings of an Angular Ball Bearing, Journal of Dynamic Systems, Measurement and Control, Vol. 32, No. 1, pp. 42-57, 2003, 10.1002/htj.10070

[8] T. Sibilli and U. Igie, Transient Thermal Modeling of Ball Bearing Using Finite Element Method, Journal of Engineering for Gas Turbines and Power, Vol. 140, No. 3, 2018, https://doi.org/10.1115/1.4037861

[9] Z. De-xing C. Weifang and L. Miaomiao, An optimized thermal network model to estimate thermal performances on a pair of angular contact ball bearings under oil-air lubrication, Applied Thermal Engineering, Vol. 131, pp. 328-339, 2018, https://doi.org/10.1016/j.applthermaleng.2017.12.019

[10] SKF, SKF Catalogue, 2018, skf.com

[11] TIMKEN Company, Angular Contact Ball Bearing Catalogue, 2019, www.timkencatalogues.com

[12] H. Herwig and A. Moschallski, Wärmeübertragung (Heat Transfer), Springer Vieweg, 3rd Edition, 2014

[13] T. L. Bergman and A. S. Lavine, Fundamentals of Heat and Mass Transfer, John Wiley and Sons, 8th Edition, 2017

[14] R. S. Burns, Advanced Control Engineering, Butterworth Heinemann, 1st Edition, 2001